Title

Underlying causes of yield spatial variability and potential for precision management in rice systems

Journal

Precision Agriculture, 14(5)

ISSN

1385-2256

Authors

Simmonds, Maegen B
Plant, Richard E
Peña-Barragán, José M
et al.

Publication Date

2013-10-01

DOI

10.1007/s11119-013-9313-x

Peer reviewed

Precision Agric (2013) 14:512–540
DOI 10.1007/s11119-013-9313-x

Underlying causes of yield spatial variability and potential for precision management in rice systems

Maegen B. Simmonds · Richard E. Plant · José M. Peña-Barragán · Chris van Kessel · Jim Hill · Bruce A. Linquist

Published online: 23 April 2013

Abstract Our current understanding of the mechanisms driving spatiotemporal yield variability in rice systems is insufficient for effective management at the sub-field scale. The overall objective of this study was to evaluate the potential of precision management for rice production. The spatiotemporal properties of multiyear yield monitor data from four rice fields, representing varying soil types and locations within the primary rice growing region in California, were quantified and characterized. The role of water management, land-leveling, and the spatial distribution of soil properties in driving yield heterogeneity was explored. Mean yield and coefficient of variation at the sampling points within each field ranged from 9.2 to 12.1 Mg ha^{-1} and from 7.1 to 14.5 %, respectively. Using a *k*-means clustering and randomization method, temporally stable yield patterns were identified in three of the four fields. Redistribution of dissolved organic carbon, nitrogen, potassium and salts by lateral flood water movement was observed across all fields, but was only related to yield variability via exacerbating areas with high soil salinity. The effects of cold water temperature and land-leveling on yield variability were not observed. Soil electrical conductivity and/or plant available phosphorus were identified as the underlying causes of the within-field yield patterns using classification and regression trees. Our results demonstrate that while the high temporal yield variability in some rice fields does not permit precision management, in other fields exhibiting stable yield patterns with identifiable causes, precision management and modified water management may improve the profitability and resource-use efficiency of rice production systems.

Keywords Food irrigation · Cluster analysis · Classification and regression trees · Soil salinity · Plant-available phosphorus

M. B. Simmonds (✉) · R. E. Plant · C. van Kessel · J. Hill · B. A. Linquist
Department of Plant Sciences, University of California, Davis, 3214 Plant and Environmental Sciences Building, Davis, CA 95616, USA
e-mail: mbsimmonds@ucdavis.edu

J. M. Peña-Barragán
Institute for Sustainable Agriculture, CSIC, 14080 Cordoba, Spain

Introduction

Rice (*Oryza sativa* L.) is a staple food source for almost half of the world population (Rice Almanac 2002). To feed the growing population in a sustainable manner will require increasing productivity of existing rice cropping systems to avoid the environmental degradation caused by the expansion of agricultural land. Increases in genetic yield potential are not keeping pace with growing food demand, calling for sustainable intensification of existing rice systems utilizing precision agriculture methodologies to narrow the gap between genetic yield potential and actual yield (Cassman 1999). Within-field spatial heterogeneity of soil properties can partly account for the yield gap (Mzuku et al. 2005; Casanova et al. 1999), yet the conventional practice in irrigated rice fields as large as 75-ha in California, is uniform management despite the availability of technology to implement precision management at the within-field scale (e.g. GPS-equipped yield monitors and variable-rate fertilizer technology). This is due to insufficient understanding of the underlying causes of yield spatiotemporal variability. An understanding of the processes shaping the yield patterns, and identification of the main yield-limiting factors across space and time are requisite for the development of precision management zones and practices.

Yield spatial variability is comprised of both permanent and transient components. In general, the persistent patterns are controlled by native field soil properties, or endogeneous factors, while the transient patterns are controlled by exogeneous factors, such as climate, pests and disease (Bakhsh et al. 2000; Basso et al. 2007; Waggoner and Aylor 2000). When these factors interact they affect yield across temporal and spatial scales, making it difficult to unravel the causes. Land-leveling and flood-irrigation practices make irrigated rice systems particularly complex due to their influence on both endogenous and exogenous factors, such as soil and water chemistry and microclimate.

Land-leveling of rice fields is done to improve water management and crop profitability, but it can also alter the magnitude and spatial variability of soil biochemical properties (Brye 2006) and yield due to the major disturbance to the soil profile caused by the redistribution of soil from high to low areas (Walker et al. 2003; Roel and Plant 2004a, b). The thickness of the relatively nutrient-rich plow layer, or Ap horizon, is reduced in "cut" areas and augmented in "fill" areas, generally resulting in distinct soil chemical properties (Walker et al. 2003). Walker et al. (2003) reported that yield declines in cut areas were strongly related to the amount of soil moved during land leveling, although they were unable to show if this was due to reduced nutrient availability.

Flood irrigation has been shown to affect the spatial and temporal variability of climate, soil chemistry and water chemistry within a rice field in three important ways: cold temperature of intake irrigation water (Raney et al. 1957), the mass flow of solutes and their evapoconcentration (Scardaci et al. 2002). In some rice fields, water temperature is not uniform due to low temperature of intake irrigation water (Raney et al. 1957). The temperature of irrigation water affects rice productivity by regulating photosynthetic and developmental rates (Shimono et al. 2004 and Shimono et al. 2002) and by influencing the susceptibility of the rice plant to spikelet sterility (Shimono et al. 2007). The threshold water temperature for yield loss is 20 °C (Roel et al. 2005).

Rice is salt-sensitive (Maas and Hoffman 1977; Shannon et al. 1998), especially during early seedling (Flowers and Yeo 1981; Maas 1990; Lutts et al. 1995) and pollination (Khatun and Flowers 1995). Scardaci et al. (2002) observed that flood water salinity and soil salinity increased from the uppermost to lowermost basins in 27 rice fields, suggesting that salts are redistributed within fields by mass flow and evapoconcentration.

Various analytical approaches have been used to reduce the complexity of spatial phenomena in agricultural fields, and to elucidate the main predictive factors of yield

variability. Various clustering procedures have been used to partition the data space of multiyear yield data space into clusters, which have the property of maximal variance among clusters and minimal variance within clusters across all years analyzed, as well as the highest probability of occurring. Lark and Stafford (1997) were the first to use fuzzy *k*-means clustering for multiyear yield monitor data to delineate management classes within fields. Using both yield and soil map data, Guastaferro et al. (2010) compared several clustering algorithms for the delineation of management zones. Roel and Plant (2004a, b) and Perez-Quezada et al. (2003) combined *k*-means clustering with randomization methods to analyze within-field yield variability. Roel and Plant (2004b) assert there are three key measures to evaluate if the clusters are physically meaningful: (1) the stability of the clusters when subject to random permutations; (2) the degree of spatial contiguity of the clusters and (3) the stability of the clusters when the number of clusters (i.e. *k*) is increased. Roel and Plant (2004a, b) found that the spatiotemporal yield variability in two rice fields could be characterized by spatially contiguous clusters (i.e. not randomly spaced), but that the degree of inter-annual variability of the average yields of each clusters differed. Thus, the authors concluded that the yield patterns were driven by edaphic properties in the field with the stable yielding clusters, and by more transient factors (e.g. climate, weeds) in the field with unstable yielding clusters. Using classification and regression trees (CART), Delmotte et al. (2011) identified weed competition as the primary yield-limiting factor in both conventional and organic rice cropping systems, while Roel and Plant (2004b) identified elevation, soil pH, clay content, soil organic matter and soil penetration resistance as the main explanatory factors for cluster membership in two rice fields.

Alternative statistical methods have been used by others to identify the primary yield-limiting factors within rice fields. Dobermann (1994) used a factor analysis and multivariate linear regression, and found that soil pH, microrelief, weed growth and seeding rate were driving yield variability. Casanova et al. (1999), using multiple regression and the boundary-line method, reported that topsoil cation exchange capacity and salinity explained the yield patterns, and calculated a yield-gap of 3,000 kg ha^{-1} due to soil factors.

Most yield variability studies in rice systems have investigated a single process hypothesized to drive within-field yield variability, such as land-leveling or water temperature, and/or a collection of soil attributes expected to be involved in yield variability. Additionally, many of the studies have been carried out in fields ranging in size from 0.5 to 3.6 ha (Yanai et al. 2001; Dobermann 1994; Casanova et al. 1999), while fewer studies exist on larger fields comprised of numerous basins.

We studied a collection of rice fields, ranging in size from 23 to 69 ha, including multiple internal basins within each field. The fields were representative of varying soil types and locations within the primary rice growing region of California. The main objective of this study was to evaluate the potential of precision management for rice production. Specifically, we sought to: (1) quantify and characterize within-field spatiotemporal variability of yield; and (2) determine underlying causes of yield variability due to water management, land-leveling and soil chemical and physical properties within fields.

Materials and methods

Site description

The experimental sites were located in four commercial rice fields (designated F1, F2, F3 and F4) in the Sacramento Valley of California. Each field was comprised of varying

numbers of sub-fields (i.e. basins) and combinations of soil types (Fig. 1 and Table 1). Field F1 contained 43-ha with five basins, located in Willows, CA (UTM Zone 10-N, coordinates 576 820 E, 4 369 898 N). Field F2 was a 69-ha field with four basins, located in Marysville, CA (UTM Zone 10-N, coordinates 622 817 E, 4 343 710 N). The F3 and F4 fields were adjacent 23-ha areas, each comprised of six basins, located on the same ranch in Arbuckle, CA (UTM Zone 10-N, coordinates 593 230 E, 4 320 325 N). All fields were managed by the cooperating growers, who implemented conventional, but field-specific, flow-through irrigation systems and applied uniform rates of fertilizers throughout the field (Table 2). Weeds and other pests were controlled as needed. The initial land-leveling events occurred 35–56 years prior to the study (Table 2). Fields were wet-seeded with pre-germinated rice seed. High yielding medium-grain rice cultivars were grown in all fields and all years (Table 2).

Field study

Soil and water sampling and yield monitoring occurred in 2008 and 2009. In addition to this data, historic yield maps were included in the analyses where available; three years of historic yield (i.e. 2005–2007) for F2 and one year of historic yield (i.e. 2007) for F4 were utilized, whereas, no historic yield data were available for F1 or F3. A geo-referenced grid sampling design was configured in each field (approximately two points per hectare), from which soil water temperature data at a subset of the points were collected. The grid points served as a common scale to compare soil properties to yield at the same locations in the field. Water samples for chemical analyses were taken from the inlets, outlets and weirs through which water flowed into each consecutive basin.

Soil data

Soil texture, depth to plow pan, pH, electrical conductivity of a saturated paste extract (EC_e), soil organic carbon (SOC), total nitrogen (N), extractable nitrate–nitrogen (NO_3–N), available phosphorus (P) and exchangeable potassium (K) were analyzed for samples from all geo-referenced grid points. All soil properties were measured in 2008 and 2009 except soil texture and depth, which were assumed to be temporally stable in the timescale of the two-year study. The rice fields in this study were originally land-leveled 35–56 years prior to the start of the experiment in 2008 (Table 2). Thus, the most significant disturbance to the soil profile occurred at that time. Annually, the fields are land-planed to maintain a level field. Soil sampling for soil texture and chemical analyses occurred in the spring, after tillage and land planing, but before fertilizer application and flooding. A composite of five sub-samples was taken from an area of approximately 5-m^2 at each geo-referenced grid point. Because the plow layer (i.e. Ap horizon) was assumed to be well-mixed from tillage, a bulk soil sample was collected from the soil surface to the depth of the plow layer. Soil samples were air-dried and after large pieces of plant debris were removed they were ground (<2 mm fraction) for textural and chemical analyses. Soil texture was determined using a Beckman-Coulter LS-230 (Miami, FL, USA) laser diffraction particle size analyzer. Soil pH was measured directly in the saturated paste using a calibrated combination electrode/digital pH meter (Burt 2004). Solution EC_e was measured in the saturation extract using a calibrated Oakton CON11 handheld conductivity/TDS meter (Vernon, IL, USA) (Burt 2004). Prior to the analyses for SOC and N determination, soil was ball-milled and carbonates were removed by acid fumigation (Harris et al. 2001). The SOC and N concentrations were measured by combustion using a PDZ Europa ANCA-GSL elemental

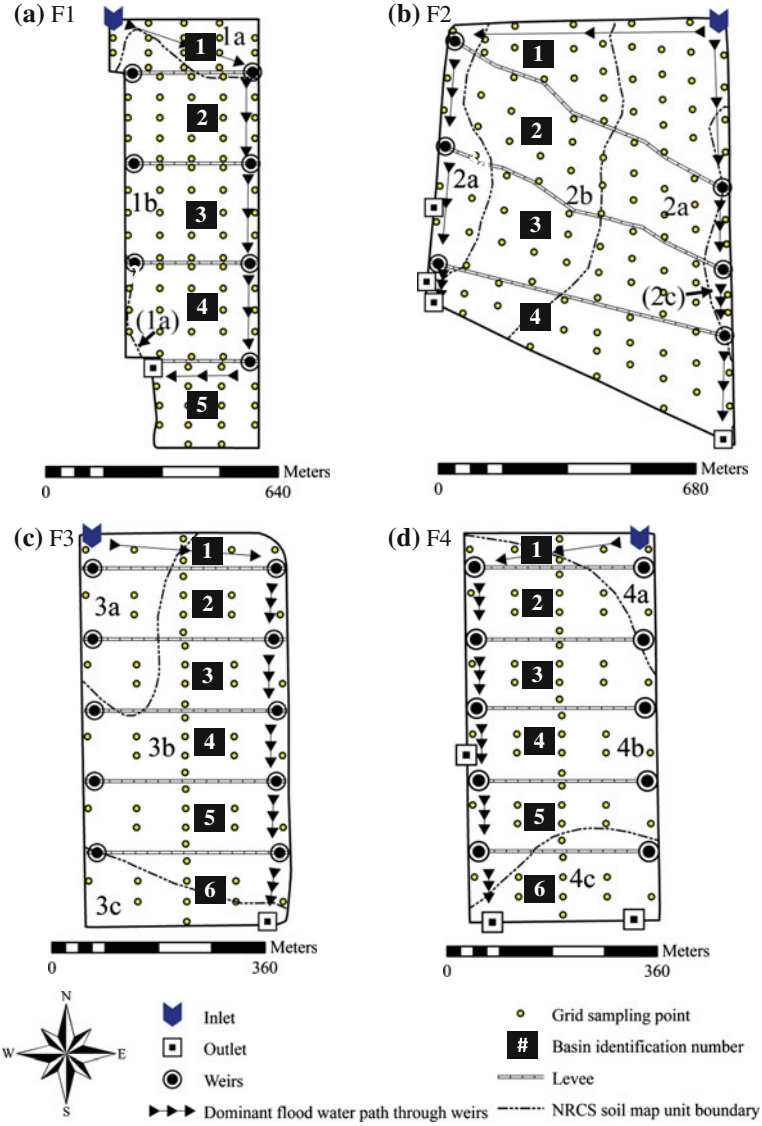

Fig. 1 Layout of the four rice fields, including the basins comprising each field, direction of the dominant path of flood water movement down the fields, and the Natural Resources Conservation Service (NRCS) soil map unit delineations and identification numbers (Table 1)

analyzer interfaced to a PDZ Europa 20-20 isotope ratio mass spectrometer (Sercon Ltd., Cheshire, UK). Soil NO_3–N concentration was determined by flow injection analyzer method (Knepel 2003). Soil P concentration was determined by sodium bicarbonate extraction buffered to pH 8.5 (Olsen and Sommers 1982). Exchangeable soil K was determined by displacement with ammonium acetate solution buffered to pH 7.0 (Thomas 1982).

Soil depth was measured after the field was flooded to obtain more accurate measurements of depth to the plow pan. A 1.2-cm diameter metal rod with a 3.3-kg weight was

Table 1 Description of the soil series and taxonomic classifications of the Natural Resources Conservation Service (NRCS) map units in the fields of the study

ID (Fig. 1)	Soil series	Taxonomic classification
1a	Willows clay, dense subsoil, slightly saline-alkali	Fine, smectitic, thermic Sodic Endoaquerts
1b	Willows clay, dense subsoil, moderately saline-alkali	Fine, smectitic, thermic Sodic Endoaquerts
2a	Kimball loam	Fine, mixed, active, thermic Mollic Palexeralfs
2b	Hollenbeck silty clay loam	Fine, smectitic, thermic Chromic Haploxererts
2c	San joaquin loam	Fine, mixed, active, thermic Abruptic Durixeralfs
3a, 4a	Vina loam	Coarse-loamy, mixed, superactive, thermic Pachic Haploxerolls
3b, 4b	Scribner silt loam	Fine-loamy, mixed, superactive, thermic Cumulic Endoaquolls
3c, 4c	Clear lake clay	Fine, smectitic, thermic Xeric Endoaquerts

used to measure the maximum depth to which a constant force penetrated the soil. Due to high variability of soil depth at each point, a Winsorized mean of five sub-samples was calculated for each location.

Water data

To determine if flood water temperature is related to spatial yield patterns, hourly surface water temperature was recorded at a subset of the grid sampling locations using Onset HOBO Pro Data Loggers (Bourne, MA, USA) from the onset of the initial flood to the final drain. Approximately three loggers per basin were installed in all basins within F1 and F2, and in the top, middle and bottom basins in F3 and F4. The loggers were secured to stakes with the temperature sensors approximately 2-cm above the soil surface, which was below the flood water surface for the majority of the growing season. In F1, F3 and F4, the flood water depth was below the temperature sensors for a maximum of four days; in contrast, F2 was drained for two weeks for an early-season herbicide application.

To determine if the spatial distribution of soil chemical properties are related to flood water movement, and subsequently yield variability, water samples were collected from the irrigation inlet, weirs that connected the individual basins and outlet(s) twice during the growing season (i.e. during the initial flood and at approximately the anthesis developmental stage of the rice) and analyzed for electrical conductivity (EC_w), dissolved organic carbon (DOC), total dissolved nitrogen (TDN), nitrate–nitrogen (NO_3–N_w), ammonium–nitrogen (NH_4–N_w), soluble phosphorus (sol-P) and soluble potassium (sol-K). Water samples were collected only from weirs with flowing water to prevent inflated concentration readings due to localized accumulation of solutes in stagnant water. Immediately after collection, water samples were stored on ice. Within 24 h, an unfiltered sub-sample from each sampling location was analyzed for EC_w using a calibrated Oakton CON11 handheld conductivity/TDS meter (Vernon, IL, USA). The other portion of the sample was filtered with a 1.2 μm glass fiber filter. Approximately half of the filtered sample was refrigerated (maximum of 5 days) until analysis for concentrations of DOC and TDN using a Shimadzu TOC-V CSN Analyzer (Kyoto, Japan). The other half of the filtered sample

Table 2 Summary of field management practices

	F1		F2[a]		F3		F4	
	2008	2009	2008	2009	2008	2009	2008	2009
Rice cultivation								
Cultivar grown[b]	M-204	M-206	M-206	M-206	M-206	M-206	M-206	M-206
Years in continuous rice prior to 2008	48		71		1[c]		1[c]	
Fertilizer and straw management								
Total N–P–K (kg ha^{-1})	163-0-0	174-21-0	195-26-0	244-38-0	181-0-0	189-0-0	181-0-0	189-0-0
Straw management	Incorporated and winter flood		Incorporated and winter flood		Incorporated		Incorporated	
Water management								
System of water management	Flow-through with minimal outflow		Flow-through with minimal outflow		Flow-through with minimal outflow in 2008 and no outflow in 2009		Flow-through with minimal outflow in 2008 and no outflow in 2009	
Dominant flow patterns	Down east side of field		Down both sides of field		Down east side of field		Down west side of field	
Land-leveling								
Approx. number of years since initial land leveling	56		35		38		38	
General direction of soil movement from initial land leveling	Northwest to southeast		Northeast to southwest		North and west-central to east and south		North and east-central to west and south	

[a] Top two basins taken out of rice production in 2009

[b] The historical yield data used from F2 included M-202 in 2005 and 2006, and M-206 in 2007, and from F4 included M-206 in 2007

[c] Rice was grown from 2003 to 2005; vineseed and beans in 2005 and 2006, respectively; and rice again from 2007-2009

was immediately frozen until further chemical analyses could be performed. In 2008, NO_3–N_w concentration was determined using a single reagent spectrophotometric method, adapted from Miranda et al. (2001) and Doane and Horwath (2003), while NH_4–N_w concentration was determined using a dual-reagent spectrophotometric method, adapted from Forster (1995) and Verdouw et al. (1978). In 2009, NO_3–N_w and NH_4–N_w concentrations were determined using a flow injection analyzer method (Knepel 2003; Hofer 2003). Soluble P (sol-P) concentration was determined according to a spectrophotometric method using Lachat Flow Injection Analyzer (Standard Methods for the Examination of Water and Wastewater (20th ed.) 1998). Soluble K (sol-K) concentration was determined by Inductively Coupled Plasma Atomic Emission Spectrometry (ICP-AES) according to EPA Method 200.7 (U.S. Environmental Protection Agency Method 2001).

Yield data

Rice was harvested using combines with global positioning system (GPS)-equipped commercial yield monitors, which were calibrated according to manufacturer's instructions prior to each harvest. Fields F3 and F4 were harvested using the same combine by the grower. Yield map data files consisted of geographic coordinates, yield and grain moisture.

Raw yield data were cleaned in five stages prior to spatiotemporal analyses: (1) Points outside of the field boundary were deleted; (2) Points with inconsistent logging intervals (i.e. >1 s) were deleted; (3) Points within 5-m of the field boundary were omitted to remove edge effects; (4) Data records with extreme yield values (<2.2 Mg ha^{-1} or >18 Mg ha^{-1}) or negative moisture values were omitted and (5) The remaining dataset was passed through a Moran Scatterplot screening process from the R package *spdep* (Bivand et al. 2010) version 0.5-21 (R statistical software, version 2.10.1). This function in turn uses the R function influence.measures to identify influential data values through a variety of statistical tests. All data values satisfying the default criteria for identification as an influential point were removed.

To obtain yield values on the same sampling grid from which soil samples were collected, the cleaned yield dataset for each field was imported into the ArcGIS, version 9.3 (ESRI, Redlands, CA, USA), geographic information system (GIS). We tested several methods for estimating yield at the grid points and chose the method having the highest correlation with all the other methods. The method we chose utilized the Spatial Analyst tool in ArcGIS to interpolate the yield data using the ordinary kriging method and then averaged the kriged yield surface within a 5-m radius of each grid point. Finally, yield data were centered and scaled for each field and year combination.

Data analysis

To evaluate whether flood irrigation practices drive yield heterogeneity through cold temperature of intake water and/or redistribution of soil nutrients and salts by flood water movement and evapoconcentration, a trend analysis was performed using R statistical software, version 2.10.1. Simple linear regression was used to model the change in (a) two flood water temperature parameters using a threshold temperature identified by Roel et al. (2005) for California rice (i.e. total number of hours below 20 °C and inverse degree days below 20 °C); (b) water chemical properties (i.e. EC_w and solute concentrations of DOC, TDN, NO_3–N_w, NH_4–N_w, sol-P and sol-K) and (c) soil chemical properties (i.e. EC_e and concentrations of SOC, N, NO_3–N, P and K) with increasing distance from the inlet. Distance from the inlet (DIST) was calculated for each sampling location as the average of

the possible path distances through the weirs to the point where the water or soil sample was collected. With respect to water chemical data, if a weir was closed during a sampling event, it was not considered as a possible route in the distance calculation. Due to the spatial nature of the dataset, assumptions of regression analyses were not met. Therefore statistical significance for each linear model was determined using an algorithm that generated a random permutation of each response variable and corresponding slope (β_1), simulated 10,000 times, wherein the fraction of permutations with a β_1 value more extreme than the observed value was taken to be the p value of the null hypothesis that $\beta_1 = 0$.

i.e. $p = \frac{\sum_{i=1}^{n} \beta_{1,i}}{n}$, where n = no. of simulations,

$$\beta_i = \begin{cases} 1 \text{ if the simulated slope is greater than the actual slope} \\ 0 \text{ if the simulated slope is less than the actual slope} \end{cases}$$

To identify and determine the underlying causes of the most spatially and temporally stable homogenous yield patches within each field, a procedure using *k*-means clustering and CART, adapted from Roel and Plant (2004b), was applied to the dataset. The *k*-means cluster algorithm was performed using the R package *e1071* version 1.6 (Dimitriadou et al. 2010). The aim of this procedure was to identify physically meaningful clusters that would serve as the response variable in the CART analysis (Roel and Plant 2004b). There was no statistic that would allow a comparison of the temporal yield variability across fields due to varying number of years of yield data available for each field. Therefore, yield temporal variability was evaluated visually by examining the stability of the mean scaled yield of the clusters over time. Fields F1 and F3 had 2 years (2008–2009), F2 had 4 years (2005–2008) and F4 had 3 years (2007–2009) of yield data available. Yield data from 2009 in F2 were excluded, as the top two basins were converted from rice production to a wildlife preserve. Prior to the CART analysis, a correlation analysis was performed using JMP version 9.0.0 (SAS Inst. Inc., Cary, NC, USA) to evaluate the stability between 2008 and 2009 observations of soil chemical properties. A CART analysis was performed using the R package *rpart* version 3.1-45 (Therneau and Atkinson 2009). In this step, the yield clusters were the response variable and the soil parameters and DIST were the explanatory variables.

The selection procedure for the optimal size of the classification tree was carried out in three steps: (1) *rpart* was replicated ten times, producing ten random rearrangements of the cross-validation training set with ten cost-complexity (cp) tables; (2) using the "1 SE rule" (Therneau and Atkinson 2009) for each table, the tree size corresponding to the lowest cp value and with a cross-validation relative error <1 standard error greater than the lowest value of the cross-validation estimate of the relative error was chosen for that replication and (3) the smallest tree of the ten replications was chosen as the optimal tree size.

Results

Temporal stability and descriptive statistics of soil properties

The correlation analysis between 2008 and 2009 soil chemical data at all grid points in each field indicates that soil chemical properties were generally temporally stable in all fields (Table 3). The Pearson rank correlation coefficients (r) for all soil properties were $\geq$0.29 except for N in F2 which was not significantly correlated between years. Since soil

Table 3 Temporal correlation of field soil properties measured in 2008 and 2009 represented by Spearman rank correlation coefficients (r) based on 95, 51, 57, and 57 samples, in F1, F2, F3 and F4, respectively

Field	SOC	N	NO_3–N	P	K	pH	EC_e
F1	0.35	0.41	0.39	0.95	0.72	0.91	0.87
F2[a]	0.29		0.49	0.95	0.72	0.76	0.44
F3	0.65	0.57	0.60	0.96	0.94	0.94	0.86
F4	0.51	0.73	0.75	0.95	0.87	0.89	0.87

The higher the value of r, the lower the temporal variability. Only significant values are shown ($p < 0.05$)

[a] Based on the bottom two basins only due to the top two basins being taken out of rice production in 2009

data were stable (Table 3), only 2008 summary statistics are presented to simplify the characterization of field soil properties (Table 4).

The degree of in-field variability of measured soil properties depended on the property and, in some instances, the field (Table 4). Soil NO_3–N, P and EC_e varied the most in all fields (CV range, 24.0–72.6 %) except F2, in which NO_3–N, P and K were most variable. Soil K was also moderately variable in F1, F3 and F4 (CV range, 16.1–22.1 %). The SOC, N and soil depth were moderately variable in all fields (CV range, 11–21.1 %), while pH varied the least (CV range, 1.82–6.61 %). Silt was the least variable of the particle size fractions in all fields (CV range, 2.4–4.9 %).

Water and soil properties in relation to flood water movement

A significant spatial relationship between flood water temperature and DIST was detected in F1, F2 and F4 ($p < 0.05$) (Table 5). In F1 and F4, flood water temperature was highest in the uppermost basins near the inlets, whereas temperature was lowest closest to the inlet in F2 in 2008 only.

Solute concentrations in flood water, most notably DOC, TDN and sol-K, generally increased as water moved towards the outlets in all fields during the initial flooding event (Table 6). For example, in 2008 flood water DOC, TDN and sol-K concentrations in F1 increased by 2.79, 0.44 and 0.90 mg L^{-1}, respectively, from the inlet to 1 000-m down the field (i.e. approximately to the bottom of the lowermost basin 5) (Table 6; Fig. 1). The greatest increases in DOC, TDN and sol-K concentrations were observed in F3 in 2008; DOC, TDN and sol-K concentrations increased by 7.44, 1.95 and 1.04 mg L^{-1}, respectively, from the inlet to 1 000-m down the field (i.e. approximately to the lowermost basin 6) (Table 6; Fig. 1). Additionally, in four of the eight field and year combinations, EC_w increased with increasing DIST (Table 6).

During the anthesis stage of the rice plant, the trend in observed flood water chemistry was less consistent across all fields (Table 7). Similar to the initial flood, DOC concentrations increased with increasing DIST, but this trend was only significant in four of the eight field and year combinations (Tables 6; 7). Mean DOC and EC_w increased from the initial flood to anthesis (i.e. 2.33 to 3.91 mg L^{-1} and 0.149 to 0.276 dS m^{-1}, respectively), while TDN and sol-K decreased (i.e. 0.37 to 0.15 mg L^{-1} and 1.57 to 0.65 mg L^{-1}, respectively) (Tables 6, 7).

In parallel to the flood water trend analysis, soil chemistry at the grid points in each field were analyzed in relationship to DIST (Table 8). Except for F1, in all fields SOC, N, P and

Table 4 Univariate statistics of soil characteristics in F1, F2, F3 and F4 in 2008 based on 95, 111, 57, and 57 samples, respectively

Field	Statistic	SOC (g kg^{-1})	N (g kg^{-1})	NO_3–N (mg kg^{-1})	P (mg kg^{-1})	K (mg kg^{-1})	pH	EC_e (dS m^{-1})	Depth[a] (cm)	Clay[a] (%)	Silt[a] (%)	Sand[a] (%)
F1	Mean	16.81	1.77	3.46	11.6	209	6.24	0.97	16	18	54	28
	SD[b]	2.712	0.22	1.17	2.78	36.1	0.36	0.26	2.0	1.3	1.5	2.2
	CV[c]	16.13	12.7	33.9	24.0	17.3	5.77	27.3	12	7.0	2.8	7.8
	Min[d]	10.23	1.26	1.00	6.80	160	5.47	0.56	12	15	49	22
	Max[e]	23.36	2.33	7.60	20.4	503	7.07	1.60	22	21	58	36
F2	Mean	17.43	1.39	2.06	27.3	126	4.80	0.34	12	14	51	35
	SD[b]	2.064	0.16	1.50	8.29	33.3	0.09	0.05	2.1	1.6	2.5	3.7
	CV[c]	11.84	11.3	72.6	30.3	26.5	1.82	14.5	17	11	4.9	11
	Min[d]	11.97	0.79	0.30	13.9	76.0	4.64	0.25	6.9	11	44	29
	Max[e]	22.37	1.69	8.30	49.1	213	5.06	0.50	18	18	56	45
F3	Mean	11.67	1.02	1.18	8.44	164	7.07	2.14	14	22	56	21
	SD[b]	1.871	0.18	0.40	4.17	26.4	0.37	1.13	1.8	3.1	2.1	4.5
	CV[c]	16.04	17.7	34.1	49.4	16.1	5.27	52.8	13	14	3.8	21
	Min[d]	6.085	0.66	0.09	3.20	117	6.29	0.54	7.3	16	50	13
	Max[e]	16.55	1.37	1.90	18.1	210	7.63	5.11	19	27	60	33
F4	Mean	11.32	1.00	1.06	6.51	169	6.97	1.13	14	21	57	22
	SD[b]	1.83	0.21	0.44	2.70	37.4	0.46	0.79	1.5	2.8	1.4	3.8
	CV[c]	16.19	21.1	41.2	41.5	22.1	6.61	70.1	11	14	2.4	17
	Min[d]	6.71	0.61	0.30	2.80	117	6.08	0.58	12	15	53	17
	Max[e]	14.69	1.34	2.00	12.6	375	7.95	4.84	18	25	59	32

[a] Measured in 2008 only

[b] Standard deviation

[c] Coefficient of variation = (SD/Mean)*100

[d] Minimum

[e] Maximum

Table 5 Change in flood water temperature parameters with increasing distance from the inlet

Field	Years	N[a]	TNHB[a]	IDD[b] (Change in temperature parameter per m)	TNHB-4w[c]	IDD-4w[d]
F1	2008	13	0.27	−1.18	0.02	−0.23
F1	2009	8		−0.35	0.02	−0.21
F2	2008	13		0.25	−0.03	0.20
F2[e]	2009	5				
F3[f]	2008	8			NA	NA
F3	2009	9				
F4	2008	8	0.09			
F4	2009	9	0.34	−0.60		

A β_1 value indicates a significant relationship ($p < 0.05$)

[a] Total number of hours below 20 °C from initial flood to final drain

[b] Inverse degree days below 20 °C from initial flood to final drain; $IDD(j) = \sum_{i=1}^{24}(T_{wj} - 20)^{-}$, where T_{wj} is the water temperature at hour i, and the operation $()^{-1}$ is defined for x ≥ 0 as $(x)^{-1} = x$, and for x < 0 as $(x)^{-1} = 0$ (Roel et al. 2005)

[c] Total number of hours below 20 °C for the 4 weeks following the initial flood

[d] Inverse degree days below 20 °C for the 4 weeks following the initial flood

[e] Excludes the top two basins in 2009

[f] Data loggers failed during the first 4 weeks of the growing season

Table 6 Change in concentration of flood water solutes with increasing distance from the inlet during the initial flood

Field	Years	N[b]	DOC	TDN	NO_3–N_w	NH_4–N_w	Sol-P	Sol-K	EC_w (Change in dS m^{-1} 1,000 m^{-1})
					(Change in mg L^{-1} 1,000 m^{-1})				
		Mean[a]	2.33	0.37	0.09	0.08	0.03	1.57	0.149
F1	2008	10	2.79	0.44		0.13	−0.02	0.90	
F1	2009	6	2.55		−0.07			0.46	
F2	2008	9	1.35	0.10				0.28	−0.009
F2[c]	2009	5	2.46	0.23	0.04	0.02		0.50	−0.016
F3	2008	5	7.44	1.95	0.49	0.28	0.03	1.04	0.129
F3	2009	8	2.45	0.43	0.09				0.082
F4	2008	5				0.08		0.57	0.024
F4	2009	7	1.78	0.25	0.04				0.028

A β_1 value indicates a significant relationship ($p < 0.05$)

[a] Mean values across all fields and both years

[b] Sample size

[c] Excludes the top two basins in 2009

K either increased in concentration with DIST or no significant relationship was observed (Table 8). In F1, only decreasing trends in soil chemical properties with increasing DIST were observed (Table 8).

Table 7 Change in concentration of flood water solutes with increasing distance from the inlet during approximately the anthesis stage of the rice

Field	Years	N[b]	DOC	TDN	NO_3–N_w	NH_4–N_w	Sol-P	Sol-K	EC_w
			(Change in mg L^{-1} 1,000 m^{-1})						(Change in dS m^{-1} 1,000 m^{-1})
		Mean[a]	3.91	0.15	0.09	0.06	0.03	0.65	0.276
F1	2008	9	2.69		−0.27		−0.02		0.020
F1	2009	7			−0.03				
F2	2008	9	0.56					−0.11	0.007
F2[c]	2009	5						−2.12	
F3	2008	4				−0.07		−0.51	0.038
F3[d]	2009	1	NA	NA	NA	NA	NA	NA	NA
F4	2008	4	2.92	−0.34	−2.12		−0.12	−0.46	0.027
F4	2009	3	4.74	0.16		0.04		−0.45	

A β_1 value indicates a significant relationship ($p < 0.05$)

[a] Mean values across all fields and both years

[b] Sample size

[c] Excludes the top two basins in 2009

[d] Missing data due to weirs being closed during the sampling event

Table 8 Change in pre-season soil chemical properties measured at grid points with increasing distance from the inlet

Field	Years	SOC	N	NO_3–N	P	K	EC_e
		(Change in g kg^{-1} 1,000 m^{-1})		(Change in mg kg^{-1} 1,000 m^{-1})			(Change in dS m^{-1} 1,000 m^{-1})
F1	2008	−1.50			−1.47		
F1	2009			−0.47	−1.78	−7.39	
F2	2008	0.96	0.05	0.81	6.21	32.81	0.04
F2[a]	2009				19.91		
F3	2008		0.31	0.27	2.78	43.84	
F3	2009	3.58	0.14	0.71	2.27	31.57	
F4	2008	1.64	0.35	−0.53	3.25	51.98	−0.86
F4	2009	5.27	0.19	−0.92	3.02	52.59	−0.57

A β_1 value indicates a significant relationship ($p < 0.05$)

[a] Excludes the top two basins in 2009

Yield temporal and spatial variability: univariate statistics and cluster analysis

The yield point data provided by the yield monitors were used to quantify and characterize the within-field yield spatiotemporal variability. In all fields, the mean interpolated yield at the grid points varied < 3 % of the mean yield of the whole field (Table 9). Whole field yield monitor data ranged from 6.52 to 16.85 Mg ha^{-1} and from 6.13 to 16.34 Mg ha^{-1} across all fields in 2008 and 2009, respectively (Table 9). To aid in visualization of the relationship between the clusters and yield, the interpolated yield at the grid points was drawn using Thiessen polygons for each field and year used in the cluster analysis (Figs 2a,

Table 9 Comparison of yield monitor univariate statistics of grain yield, at 14 % moisture content, of the whole field verses interpolated at the grid points in Fields 1–4 (F1–F4) in 2008 and 2009

Field	Statistic	Yield monitor			
		Whole field[a] (Mg ha^{-1}) 2008	Grid points[b] (Mg ha^{-1}) 2008	Whole field[a] (Mg ha^{-1}) 2009	Grid points[b] (Mg ha^{-1}) 2009
F1	Mean	10.50	10.63	12.33	12.12
	SD[d]	1.69	1.11	1.65	0.90
	CV[e]	16.08	10.48	13.37	7.42
	Min[f]	6.52	7.69	7.83	9.83
	Max[g]	14.20	13.09	15.95	13.77
F2	Mean	10.54	10.28	9.21	9.24
	SD[d]	0.93	0.73	1.42	1.34
	CV[e]	8.81	7.09	15.37	14.48
	Min[f]	8.09	7.73	6.13	6.69
	Max[g]	12.48	11.82	12.14	12.04
F3	Mean	10.41	10.54	10.78	11.05
	SD[d]	1.70	1.10	1.68	1.03
	CV[e]	16.29	10.41	15.63	9.31
	Min[f]	6.86	8.32	6.87	8.93
	Max[g]	16.44	13.97	15.28	13.08
F4	Mean	10.85	10.82	11.38	11.30
	SD[d]	1.82	1.05	1.89	1.10
	CV[e]	16.73	9.69	16.63	9.69
	Min[f]	6.62	8.15	6.30	8.38
	Max[g]	16.85	14.41	16.34	13.56

[a] F1 $n = 59\,633$ in 2008 and $n = 59\,664$ in 2009; F2 $n = 81\,154$ in 2008 and $n = 38\,442$ in 2009; F3 $n = 23\,056$ in 2008 and $n = 20\,961$ in 2009; F4 $n = 21\,979$ in 2008 and $n = 17\,746$ in 2009

[b] F1 $n = 95$ in 2008 and 2009; F2 $n = 111$ in 2008 and $n = 51$ in 2009; F3 $n = 57$ in 2008 and 2009; F4 $n = 57$ in 2008 and 2009

[c] F1 through F4 $n = 15$ in all years with the exception of F2 $n = 10$ in 2009 and F4 $n = 13$ in 2009

[d] Standard deviation

[e] Coefficient of variation

[f] Mean of bottom 3 % of data records for whole field or the actual minimum value for grid points

[g] Mean of top 3 % of data records for whole field or the actual minimum value for grid points

3a, 4a, 5a). With respect to the whole field, yield variability was most evident in F1, F3 and F4 (CV range, 16.08–16.73 %) compared to F2 (CV, 8.81 %) in 2008 (Table 9). The Moran's I statistic was computed for the grid point yield in each field and year combination used in the cluster analysis, and shows that yield was spatially autocorrelated in all instances except in F1 (Table 10). The Thiessen polygon maps of the yield clusters in each field depict the degree of the spatial relationships and contiguity of the clusters identified in the cluster analysis (Figs 2b, 3b, 4b and 5b). The optimal *k*-value for each field varied, and was decided upon in each case according to the procedure outlined by Roel and Plant (2004b).

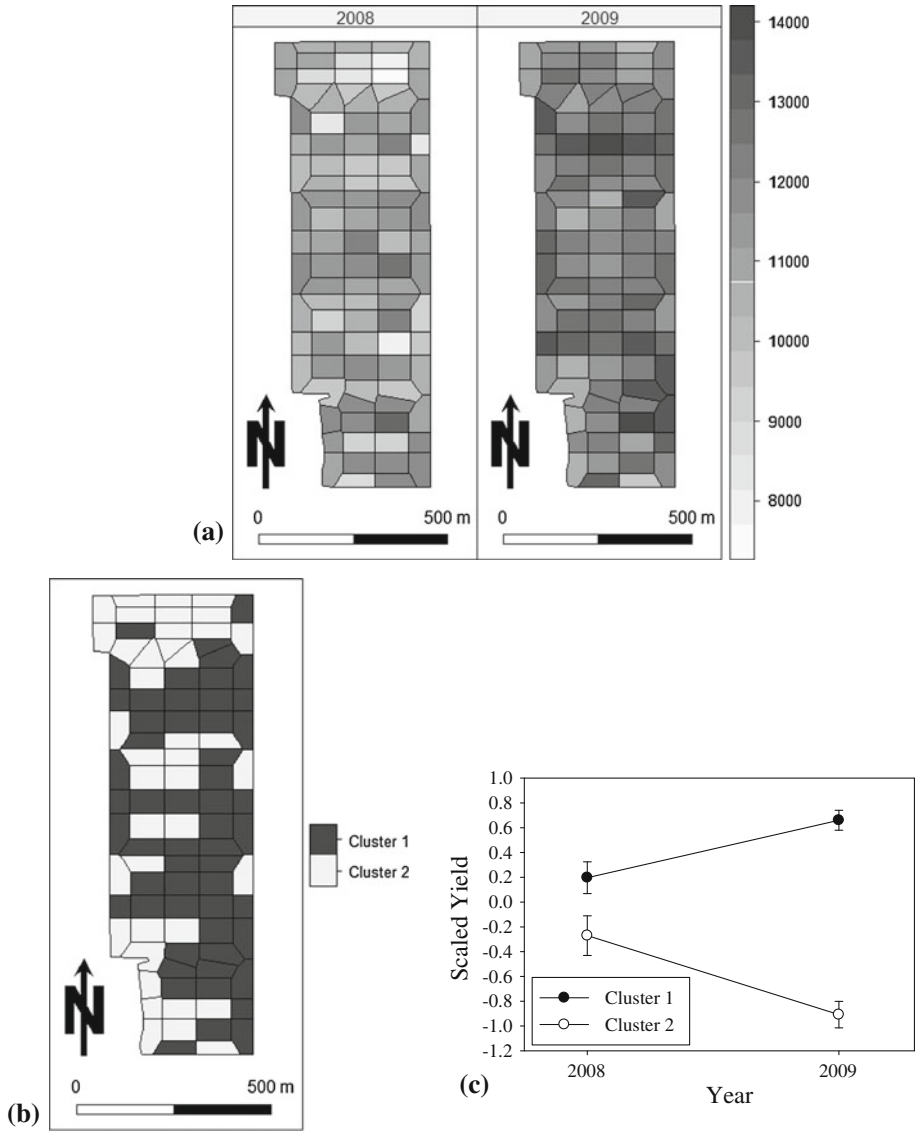

Fig. 2 **a** Interpolated yield point data (kg ha^{-1} at 14 % moisture content) in F1 presented using Thiessen polygons. **b** Cluster classifications of interpolated yield data for $k = 2$ in F1 presented using Thiessen polygons. **c** Change in the scaled, mean yield of points belonging to each cluster classification over time

In F1, $k = 2$ was used for 2008 and 2009 yield data (Fig. 2). The two clusters were temporally stable, in that over the 2 years, cluster 1 had above-average yield and cluster 2 had below-average yield (Fig. 2c). However, the yield-gap between the two clusters increased in 2009 (Fig. 2c). There were no strong spatial patterns of the clusters (Fig. 2b). Although a portion of the points belonging to the low-yielding cluster 2 were concentrated in the uppermost basin 1, and to a lesser extent, along the west field boundary in basins 4

and 5 (Fig. 2b). Additionally, the higher-yielding cluster 1 was somewhat concentrated in basin 2 and the east side of the field (Fig. 2b).

There was not a temporally stable spatial yield pattern in F2 over the 4-year period from 2005 to 2008, which is illustrated by the difference in the two cluster sets for $k = 2$; with the west side of the field a member of cluster 2 (i.e. Set 1), cluster 1 is higher yielding all years except for 2008, whereas with the west side of the field included in cluster 1 (i.e. Set 2), cluster 2 is higher yielding all years except for 2007 (Fig. 3b, c).

The cluster maps for both $k = 2$ and $k = 3$ are shown for F3 (Fig. 4b). The temporal variability of yield of the individual clusters from 2008 to 2009 was stable and consistent with increasing k-value (Fig. 4c). The first split of the data space for $k = 2$ divided it into two relatively spatially distinct regions of low and high yield (Fig. 4b). The points belonging to the low-yielding cluster 1 were concentrated in the west-central side of basins 2, 3 and 4 (Fig. 4b, c). The points surrounding this area, primarily in basin 1, basin 6 and the east side of basins 2, 3, 4 and 5, belong to the higher yielding cluster 2 (Fig. 4b, c). When k was increased from 2 to 3, the higher-yielding cluster 2 was split into the average-yielding cluster 3 and cluster 2 with above-average yield, while the lowest yielding cluster 1 remained generally intact (Fig. 4b, c).

In F4, $k = 2$ was used for 2007–2009 yield data (Fig. 5b). The temporal variability of the 2 clusters over the 3 years was generally stable and the relative yield difference between them increased with time (Fig. 5c). Generally, the north-central to east region of the field (i.e. predominately basins 2 and 3) belongs to the lower yielding cluster 1, while the southernmost portion of the field (i.e. predominately basins 5 and 6) belongs to the higher yielding cluster 2 (Fig. 5b, c).

CART analysis

For each field, the stable yield clusters identified in the cluster analysis served as the categorical dependent variable in the CART analysis, with the exception of F2 for which no stable cluster set was identified and therefore was excluded from the CART analysis. The predictor variables included DIST, to indirectly test for the effect of water management, and the soil parameters: depth, pH, EC_e, SOC, N, NO_3–N, P, K and percent clay. Percent sand and silt were omitted from the CART analysis due to redundancy if all three particle size fractions were included. Both 2008 and 2009 soil data were included in the analysis, but the years are not specified to simplify the results. If both years of a particular variable were of importance in the analysis, only the logic expression for the highest ranking year is mentioned.

In F1, for $k = 2$, a portion of the replications of the *rpart* function resulted in a cp value corresponding to 0 splits, which would not produce a tree. Using a cp value corresponding to 1 split (the next highest cp value among the replications) resulted in a partition of the field into points with "low P" (<7.75 mg kg^{-1}) and "high P" (≥ 7.75 mg kg^{-1}), corresponding to the high-yielding cluster 1 and low-yielding cluster 2, respectively (Fig. 6). With P as the primary splitting variable, 32 % of all points in F2 were misclassified, which was the highest misclassification percentage compared to F3 and F4 (Fig. 6a). The "high P" points were generally localized in both the uppermost basin 1 and the west-central area of the rest of the field. About half of the points within the high-yielding cluster 1 were misclassified as cluster 2, as they had P levels ≥ 7.75 mg kg^{-1} (Fig. 6). The top surrogate for P was EC_e. Points with "high EC_e" (≥ 0.87 dS m^{-1}) were classified as the low-yielding cluster 2 and had a spatial pattern similar to P (Fig. 6b). The in-field spatial distributions of P and EC_e levels are illustrated in Fig. 7.

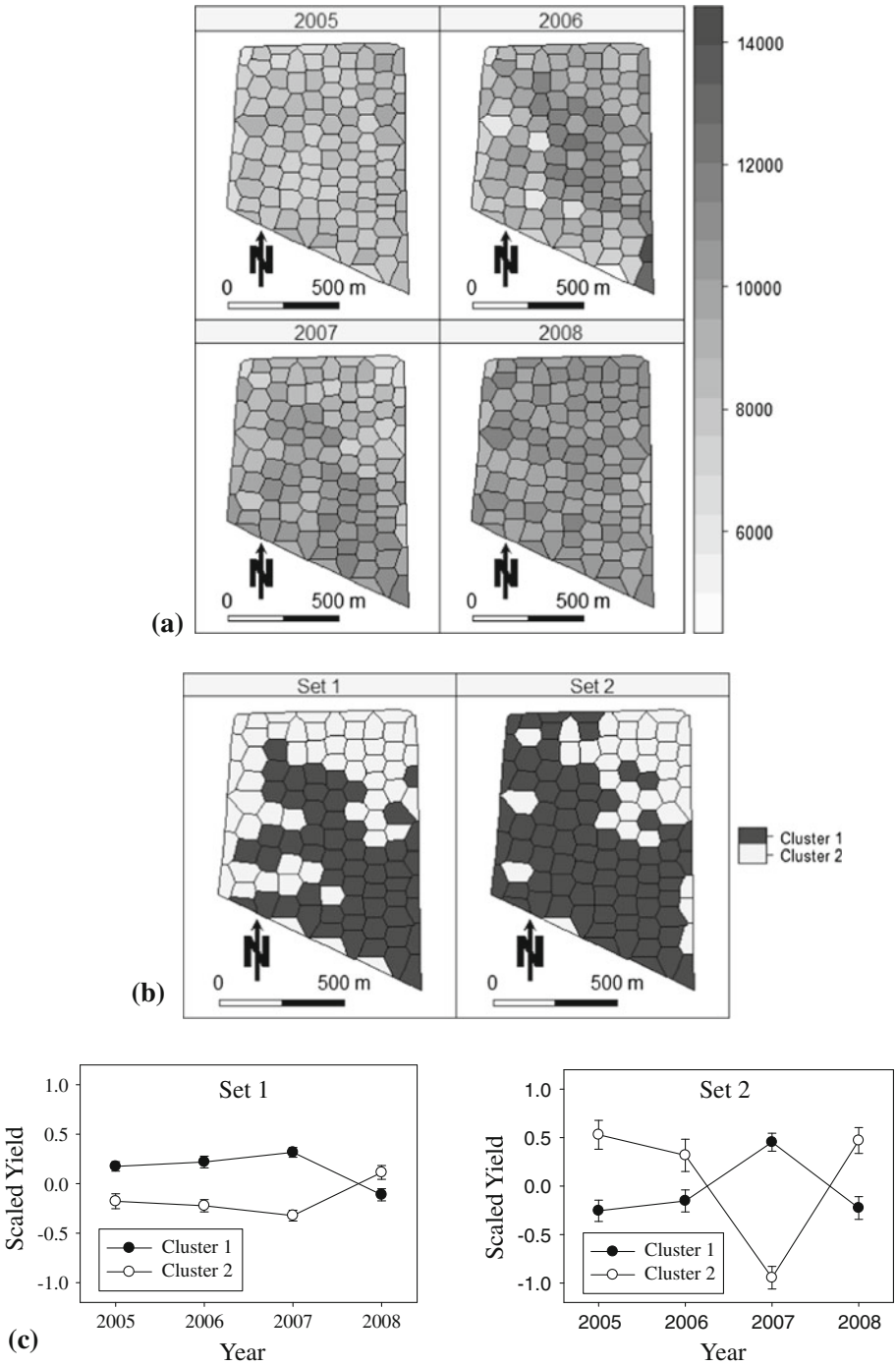

Fig. 3 **a** Interpolated yield point data (kg ha^{-1} at 14 % moisture content) in F2 presented using Thiessen polygons. **b** Cluster classifications of interpolated yield data for two cluster sets for $k = 2$ in F2 presented using Thiessen polygons. **c** Change in the scaled, mean yield of points belonging to each cluster classification over time

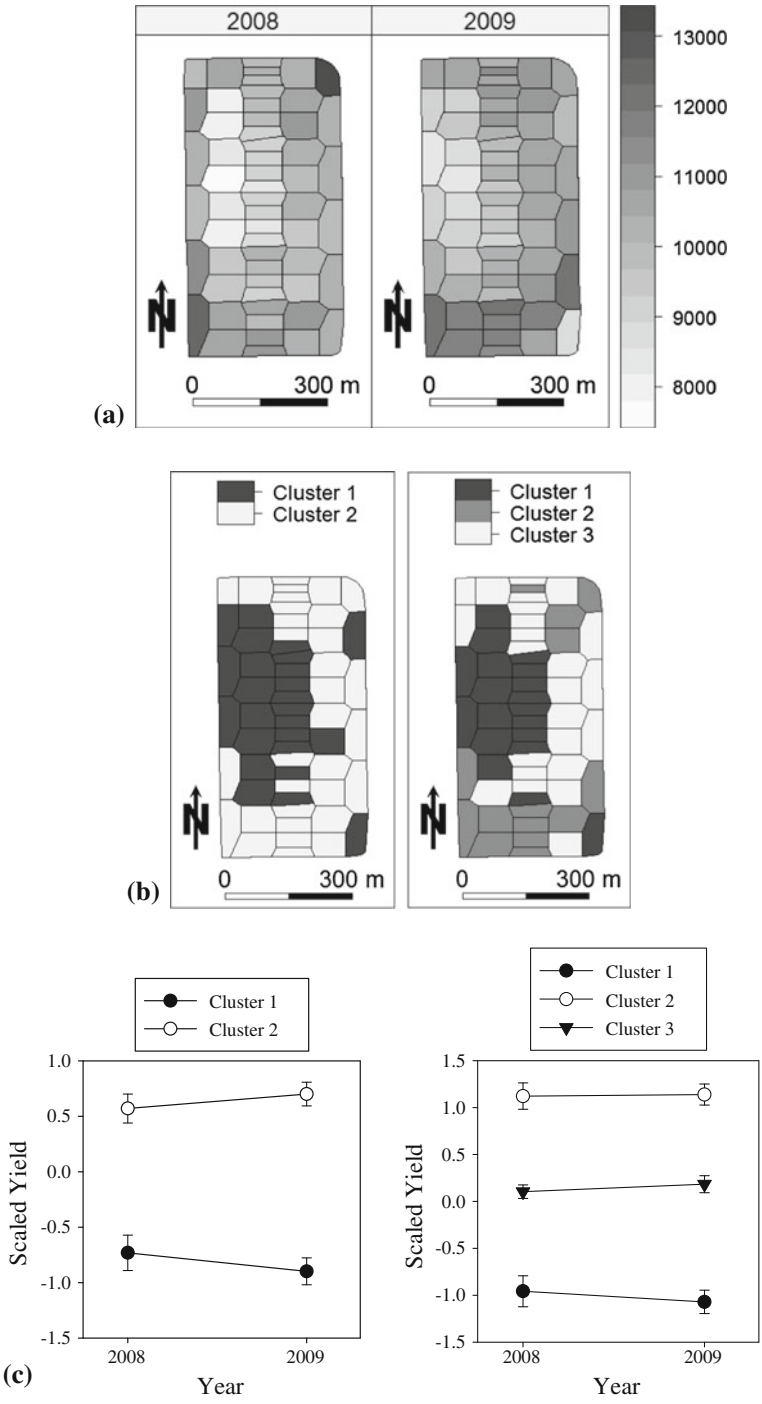

Fig. 4 **a** Interpolated yield point data (kg ha^{-1} at 14 % moisture content) in F3 drawn using Thiessen polygons. **b** Cluster classifications of interpolated yield data for $k = 2$ and $k = 3$ (*from left to right*). **c** Change in the scaled, mean yield of points belonging to each cluster classification over time

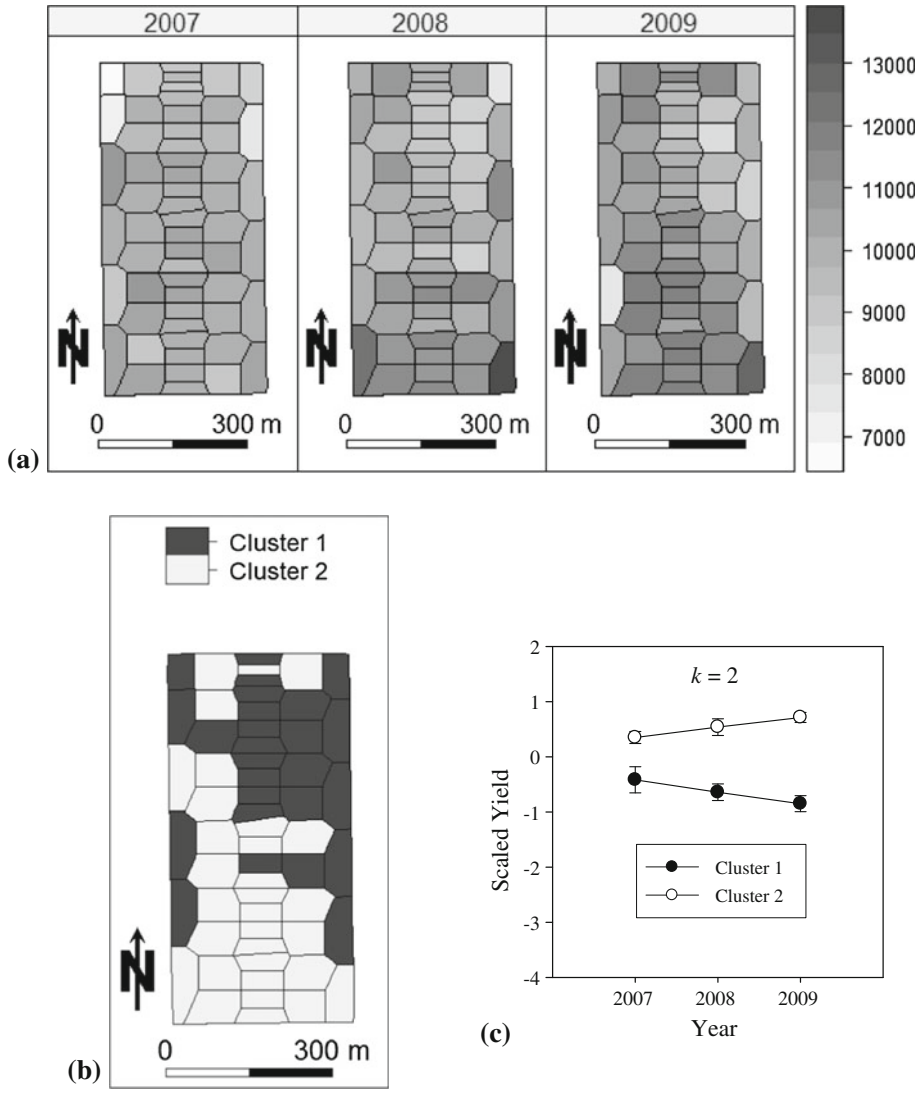

Fig. 5 **a** Interpolated yield point data (kg ha^{-1} at 14 % moisture content) in F4 drawn using Thiessen polygons. **b** Cluster classifications of interpolated yield data for $k = 2$. **c** Change in the scaled, mean yield of points belonging to each cluster classification over time

In F3, the optimal tree for $k = 2$ had 1 split with P as the primary partitioning variable and an overall misclassification of 14 % of the total points (Fig. 8a). Points with "low P" (<5.95 mg kg^{-1}) or "high P" (≥5.95 mg kg^{-1}) were classified as the low-yielding cluster 1 or the high-yielding cluster 2, respectively (Fig. 8a). The top competitor and surrogate for P was pH followed by EC_e (i.e. $EC_e \geq 2.595$ dS m^{-1} was classified as the low-yielding cluster 1). The in-field spatial distributions of P and EC_e levels are illustrated in Fig. 9.

The optimal tree for $k = 3$ in F3 had the same initial split as $k = 2$, but further divided points with "high P" (≥5.95 mg kg^{-1}) into those close to the inlet and those further away, resulting in an overall 19 % misclassification of all points (Fig. 8b). The top surrogate and

Table 10 Global Moran's I statistic and corresponding z score quantifies the degree of spatial autocorrelation of interpolated yield values at grid points within each field and year used in the cluster analysis

Field	Year	Moran's I (*z*)
F1	2008	0.10 (0.97)
	2009	0.14 (1.27)
F2	2005	0.20 (2.94)**
	2006	0.33 (4.79)***
	2007	0.55 (7.79)***
	2008	0.19 (2.78)**
F3	2008	0.40 (3.82)***
	2009	0.53 (4.91)***
F4	2007	0.26 (2.66)**
	2008	0.37 (3.58)***
	2009	0.49 (4.57)***

** $p < 0.01$, *** $p < 0.001$

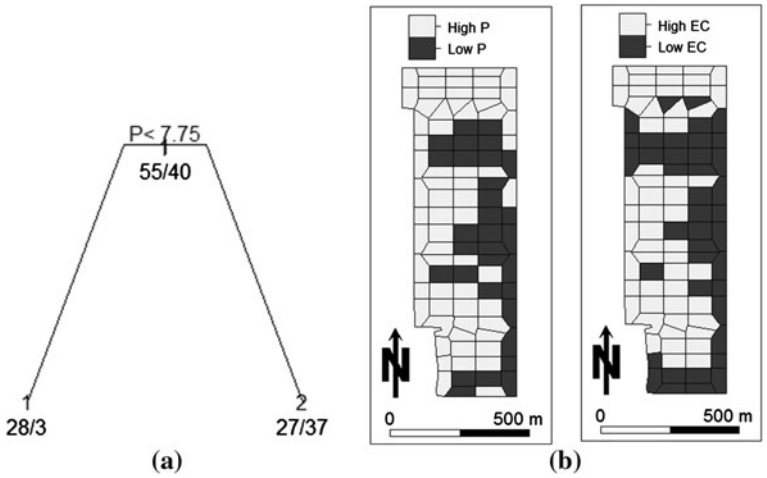

Fig. 6 **a** Classification tree obtained for $k = 2$ in F1 divides the grid points by their P concentration to predict membership into cluster 1 or cluster 2 (indicated in the *top line of the terminal nodes*). Points for which the logic statement (i.e., P < 7.75 mg kg^{-1}) is true go to the *left node*, while false points go to the *right node*. Values shown below the first splitting variable (in this tree it is P) *from left to right* indicate the initial number of elements within clusters 1 and 2, respectively. Similarly, at each terminal node the points within each partitioning category are counted by their cluster identification number. For example, in the *left node*, 28 points within cluster 1, and 3 points within cluster 2, have P < 7.75 mg kg^{-1}, and are categorized as cluster 1. **b** Maps of recursive partitioning categories for the primary splitting variable, P (*left*), and the top surrogate splitting variable, EC_e (*right*), drawn for each grid point using Thiessen polygons

competitor for DIST were K and pH, respectively. Using pH instead of DIST, points with "high P and "low pH" (<6.99) were classified as the high-yielding cluster 2 with a mean EC_e of 1.18 dS m^{-1}, while points with "high P" and "high pH" (≥6.99) were classified as the average-yielding cluster 3 with a mean EC_e of 2.08 dS m^{-1} (Figs. 8c, 9). Furthermore, the points with "low P", classified as the low-yielding cluster 1, had the highest mean EC_e of 3.07 dS m^{-1} (Figs. 8c, 9).

In F4, the optimal tree for $k = 2$ had 3 splits dependent on pH, N and SOC, resulting in the lowest overall misclassification of 8.7 % compared to F1 and F3 (Fig. 10). The

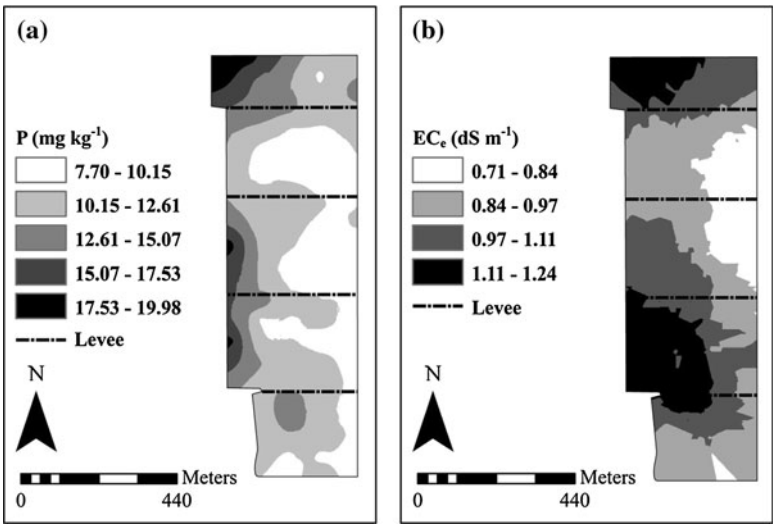

Fig. 7 Maps of interpolated soil P and EC_e grid point data in F1 from 2008 using ordinary kriging method

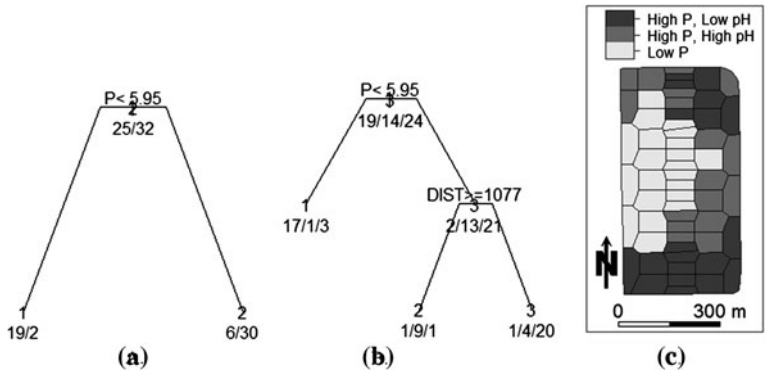

Fig. 8 **a** Classification tree for $k = 2$ in F3. **b** Classification tree for $k = 3$ in F3. **c** Recursive partitioning categories for $k = 3$ using the primary splitting variable, P, and pH, the top competitor for DIST, and drawn for each grid point using Thiessen polygons. The classification trees are interpreted the same as that of Fig. 6a

majority of the points within F4 were either partitioned into points with "high pH" ($\geq$7.05), predicting the low-yielding cluster 1, or points with "low pH and high N" ($N \geq 1.088$ g kg^{-1}), predicting the high-yielding cluster 2 (Fig. 10). Points classified as the low-yielding cluster 1 by "high pH" had the highest mean EC_e and lowest mean P (i.e. 1.72 dS m^{-1} and 4.72 mg kg^{-1}, respectively), while points classified as the high-yielding cluster 2 by "low pH and high N", had the lowest mean EC_e and highest mean P (i.e. 0.91 dS m^{-1} and 7.02 mg kg^{-1}, respectively) (Figs. 10, 11). These two recursive partitioning categories each encompassed the largest spatially contiguous areas in F4 (Fig. 10b). Among the 9 points remaining with "low pH and low N", those with "high SOC"

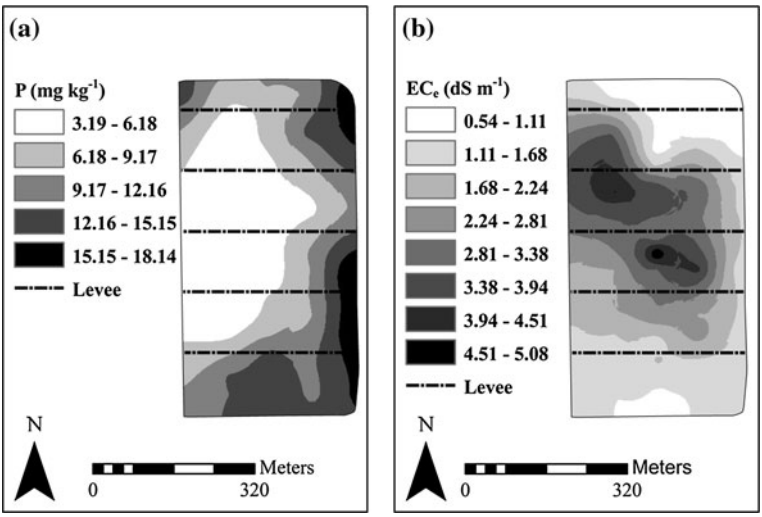

Fig. 9 Maps of interpolated soil P and EC_e grid point data in F3 from 2008 using ordinary kriging method

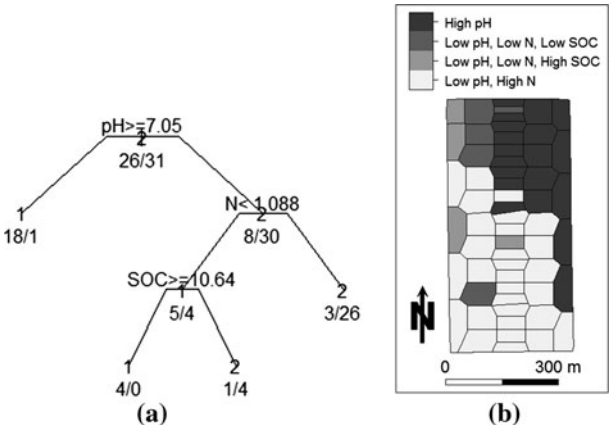

Fig. 10 **a** Classification tree for $k = 2$ in F4 is interpreted the same as in Fig. 6a. **b** Recursive partitioning categories for $k = 2$ using the primary splitting variables, pH, N and SOC, and drawn for each point using Thiessen polygons

($\geq$10.64 g kg^{-1}) were classified as the low-yielding cluster 1, and points with "low SOC" (<10.64 g kg^{-1}) were classified as the high-yielding cluster 2 (Fig. 10).

Discussion

For precision management to be beneficial in rice systems, substantial spatial variability must be identified, persist temporally and its underlying causes be understood in order to be effectively treated. Wehlan and McBratney (2000) proposed the Null Hypothesis of Precision Agriculture (NHPA) to test whether reducing the management scale of a given area would improve a set of predefined metrics, such as net profit and nutrient recovery

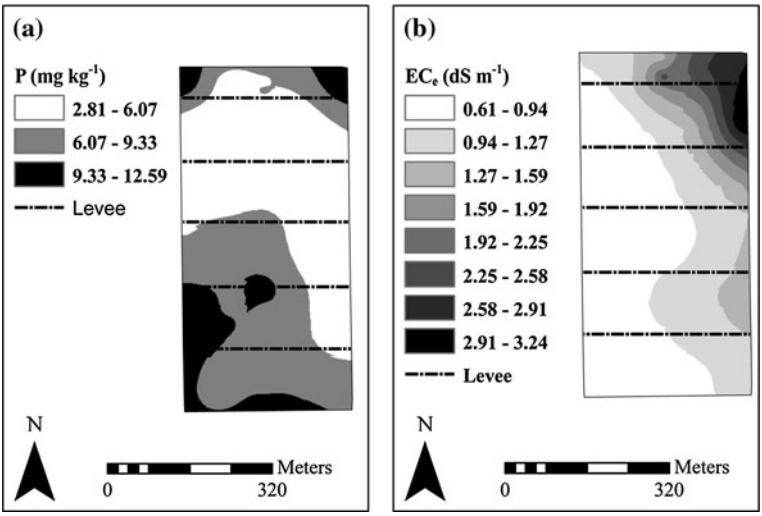

Fig. 11 Maps of interpolated soil P and EC_e grid point data in F4 from 2008 using ordinary kriging method

efficiency. However, for a real dataset it is not necessarily practical or even possible to use conventional statistical methods to test this hypothesis. The data collected in this research are observational, and are not appropriate for confirmatory statistics. Thus, in the context of this study analyzing the NHPA is an exploratory endeavor that requires rigorous quantification and characterization of spatiotemporal variability, and subjective interpretation of the results. As we acknowledge the risk of concluding a false positive (i.e. identifying a pattern or trend that is not real) in such a study, we have aimed to balance that risk with the benefit of being able to interpret how complex patterns of yield and edaphic properties change in space and time.

Yield spatiotemporal variability

The four fields investigated exhibited varying degrees of in-field variability of yield (Table 9). F1, F3 and F4 had the highest variation in yield among grid points (i.e. CV of grid points in 2008 = 10.48, 10.41 and 9.69 %, respectively) compared to F2 (CV of grid points in 2008 = 7.09 %) (Table 9). A broad range of yield variation within irrigated rice fields has been reported, but was based on considerably smaller field sizes and higher sampling density. For example, Dobermann (1994) reported a higher CV of 39 % based on 81 samples in a 3.6-ha rice field, while Yanai et al. (2001) observed much less variation in yield with a CV of 5.89 % based on 100 samples in a in 0.5-ha rice field.

Based on the cluster analysis results for each field, the temporal stability of yield patterns varied among fields, indicating that there is a spectrum of suitability of rice fields for precision management (Figs. 2, 3, 4, 5). The inconsistency in the two possible cluster sets for $k = 2$ in F2 indicates that the spatial patterns in this field have been influenced in large part by transient exogenous factors (e.g. weeds, pests, climate) as opposed to persistent endogenous factors (Fig. 3b, c). This was corroborated by the grower's observations that there was a poor stand in the northeast corner in 2007 relative to the rest of the field due to deep water and weed pressure (Figs. 3b, c, Set 2). Higher weed density occurring in

an area with deeper water is plausible, as the water may have protected the weeds from contact with a foliar active herbicide. Contrary to F2, which lacked a stable yield pattern, F1, F3 and F4 exhibited a stable and spatially contiguous yield pattern in at least a portion of each field, providing part of the evidence required to reject the NHPA (Figs 2, 4, 5).

Classification and regression tree analysis

In an observational exploratory analysis such as this, there exists a high level of multicollinearity among the suite of variables measured. Therefore, attention was given to the surrogate and competitor variables in addition to the primary partitioning variables identified in the CART analysis. Subsequently, biophysically-based interpretations were made to identify the primary factors causing yield variability in this collection of rice fields. The key yield-limiting edaphic factors explaining the stable yield patterns found in F1, F3 and F4 were EC_e and P, which in each field were the primary splitting variables, competitor and/or surrogate, and/or highly correlated to a splitting variable (Figs. 6, 7, 8, 9, 10, 11).

Maas and Grattan (1999) reported an EC_e threshold of 3 dS m^{-1} for rice. However, several lower yielding clusters within the rice fields were distinguished from higher yielding clusters by EC_e values <3 dS m^{-1}. This may be due to variation in salinity thresholds and tolerance levels among rice genotypes (Flowers and Yeo 1981; Rao et al. 2008), as well as an underestimation of EC_e due to the timing of soil sampling prior to the initial flood; Scardaci et al. (2002) observed increases in flood water salinity during the water-holding periods required after herbicide applications in rice fields, which suggests that soil samples collected prior to flooding may be less than the EC_e levels during the water holding periods. Alternatively, a variable not measured in this study may have caused the yield variability.

Soil P content below 6 mg kg^{-1} is considered to be deficient in California rice fields (Williams 2010; Linquist and Ruark 2011). Fields F3 and F4 had minimum P concentrations below the critical level (3.2 and 2.8 mg kg^{-1}, respectively) (Table 4). Although SOC, N, K and pH were in some instances correlated with the yield clusters, it is likely they were masking the effects of P and EC_e levels, which were approaching or exceeding critical levels in the low-yielding clusters. Furthermore, the fields were adequately fertilized with N, which would potentially mask deficiencies in the indigenous soil N supply. The spatial distribution of SOC and N within rice fields may be partly due to higher crop productivity and subsequent accumulation of organic matter, as opposed to the cause of the observed yield patterns. Although K was correlated with some of the yield clusters, it was not interpreted to be driving yield variability, as the minimum K concentration measured in F1, F3 and F4 was 117 mg kg^{-1}, which is well above the published critical level of 60 mg kg^{-1} in California rice soils (De Datta and Mikkelson 1985) (Table 4). However, the movement of K down the fields by mass flow in the flood water may over time necessitate K fertilization in the uppermost basins (Table 6).

In F1, P was unexpectedly negatively correlated with yield and surfaced as the primary partitioning variable of the two yield clusters (Fig. 6). This anomaly can be explained by the positive correlation among P, pH and EC_e in this particular field. Subsequently, the low-yielding areas were correlated with both high EC_e and high P in this field (Figs. 2, 6, 7). Additionally, it may be the case that P has been depleted in higher-yielding areas due greater removal of P in plant biomass. This suggests P was a masking variable in the CART analysis in F1, and EC_e, the top surrogate for P, offered the more logical explanation for the low-yielding cluster. The tree with EC_e as the partitioning variable classified the low-

and high-yielding clusters based on EC_e above or below 0.87 dS m^{-1}, respectively (Fig. 6).

In F3 and F4, high EC_e and low P were identified as driving the division between the low- and high-yielding clusters (Figs. 8, 9, 10, 11). In F3, the low-yielding cluster 1 for $k = 3$, located in a single, spatially contiguous area and mainly within basins 3 and 4, was elucidated by P < 5.95 mg kg^{-1} in the CART analysis, which coincides with the critical soil P content of 6 mg kg^{-1} in California rice fields (Williams 2010; Linquist and Ruark 2011) (Fig. 8, 9). Soil pH and EC_e were the top surrogates and competitors for P in F3. In irrigated rice soils, pH is generally not considered to limit yield due to the tendency for pH to equilibrate close to pH of 7 in flooded conditions regardless of the initial pH of the non-flooded soil. Therefore, attention was given to EC_e as a potential surrogate or co-limiting factor in F3 (Fig. 9b). The classification of the low- and high-yielding clusters was based on an EC_e value above or below 2.015 dS m^{-1}, respectively. The factor underlying the two higher yielding clusters in F3 with P ≥ 5.95 mg kg^{-1} was DIST, which indicated that there was a bio-physical explanation for the difference between the clusters that was related to the proximity to the inlet. The top competitor for DIST was K, but all K levels throughout the field were well above the critical level of 60 mg kg^{-1} for California rice soils (De Datta and Mikkelson 1985) (Table 4). For comparison, pH, the next top competitor for DIST, was highly positively correlated with EC_e, which was known to be problematic in this field (Fig. 9b). Although EC_e was not a competitor or surrogate for DIST, it corresponded to the difference in mean yield of the two clusters; relative to cluster 2, cluster 3 was lower yielding and the points classified as cluster 3 in the CART analysis had a higher mean EC_e of 2.08 dS m^{-1} compared to the points classified as cluster 2, which had a mean EC_e of 1.18 dS m^{-1} (Figs. 8c, 9b).

A similar interpretation of the classification tree obtained for F4 is made, as EC_e was one of the top surrogates for pH, which primarily divided the field into the low-yielding cluster 1 based on pH ≥ 7.05, and into the high-yielding cluster 2 based on pH < 7.05 (Fig. 10). The points classified as the low-yielding cluster 1 had the highest mean EC_e of 1.72 dS m^{-1} (Figs. 10, 11). Furthermore, the same set of points classified as cluster 1 also had the lowest mean P (4.72 mg kg^{-1}), which is below the critical P level of 6 mg kg^{-1} (Williams 2010; Linquist and Ruark 2011), while the points classified as the high-yielding cluster 2 by "low pH and high N" had the lowest mean EC_e (0.91 dS m^{-1}) and highest mean P (7.02 mg kg^{-1}) (Figs 10, 11).

The effect of land-leveling on rice yield variability reported by Walker et al. (2003) and Roel and Plant (2004b) was not observed, as the CART analysis did not indicate soil depth was driving the spatial yield patterns in any of the fields (Figs. 6, 8, 10). Possible reasons for lack of an apparent relationship between the initial land-leveling event and yield variability are that the field equilibrated to the climate and management practices over the considerable amount of time (i.e. ≥35 years) since the field was first land leveled (Eck 1987) (Table 2). For example, the spatial distribution of EC_e levels in F1, F3 and F4 may actually be the result of saline sub-soil that was exposed by the initial land-leveling process, but the EC_e patterns may no longer be correlated with soil depth (Figs. 7, 9, 11).

Role of water management in spatial variability of soil properties and yield

Unlike other studies (Roel et al. 2005; Raney et al. 1957), we did not observe a significant effect of cold water temperature on rice yield variability (Table 5). Despite periods of water temperature below the reported threshold of 20 °C for rice (Roel et al. 2005), the

mean hourly water temperature across the entire growing season at all locations was above 20 °C (data not shown).

Similar to the findings of Scardaci et al. (2002) wherein salinity was significantly higher in lowermost basins of various rice fields relative to the uppermost basins nearest the inlets, valuable soil nutrients (i.e. N and K), as well as DOC and salts in general (i.e. EC_w), were redistributed via mass flow in irrigation water down the fields and subsequently deposited in the lowermost basins or in areas with low lateral water movement by evapoconcentration (Fig. 1; Tables 6, 7, 8). Nutrient loss in the uppermost basins due to water movement has not yet affected yield based on the interpretations of the cluster and CART analyses in relation to the spatial orientation of the basins and water management practices. However, the redistribution of soil nutrients down a field may in the long-term reduce yield potential in the uppermost basins, and in areas where water movement is restricted, reduce yield due to the accumulation of salts. Indeed, low-flow areas corresponded in general to low-yielding clusters in F1, F3 and F4, which were differentiated from high-yielding clusters partly by elevated EC_e (Figs. 1, 7b, 9b, 11b). Thus, yield variability may already be affected and/or exacerbated by water management. For example, the relatively high EC_e areas located in the west side of basins 3 and 4 in F1 belong to the low-yielding cluster 1, which may be influenced by water management; the dominant water flow patterns were down the east side of F1 with minimal water flow through the west side of the field, favoring salt accumulation on the west side of the field (Figs. 1, 7b). The low-yielding areas in F3 and F4, explained partly by high EC_e in the CART analysis, may primarily be due to pre-existing soil conditions. However, historical water management practices in F3 and F4 favored water flow down the east and west sides of the fields, respectively, which would have exacerbated the yield-limiting salinity problems observed in these fields (Figs. 1, 9b, 11b).

Conclusions

Analyzing the in-field spatial yield patterns, their stability and underlying causes is a critical first step in evaluating the appropriateness of precision management relative to field-scale (i.e. uniform) management in flood-irrigated rice systems. This study demonstrated that the suitability of California rice fields for precision management must be evaluated on a case-by-case basis due to high temporal variability of spatial yield patterns observed in some rice fields (i.e. F2) and stable yield patterns with identifiable causes (i.e. EC_e and P) observed in other fields (i.e. F1, F3 and F4). The latter scenario may benefit from precision management, as well as adjustments in water management.

The redistribution of N and K by flood water movement down the rice fields was a commonality observed across all fields, which has important long-term implications for development of plant nutrient deficiencies in the uppermost basins. Although this redistribution is not affecting yield yet, uppermost basins may become separate management zones in the future. While it is uncertain whether the spatial EC_e patterns observed in F1, F3 and F4 were due to the transport and subsequent accumulation of salts in low-flow areas, or due to pre-existing soil properties, it is certain that the historical water management practices that favored water flow down a single side of the field exacerbated the problem. Water management that promotes flushing salts out of a field (e.g. allowing irrigation water to flow down both sides of the field, alternating flow patterns interannually, and/or flooding fields in the winter) may help ameliorate the salinity problems associated with the low-yielding zones.

More traditional precision management practices that may increase profitability of irrigated rice fields with spatially and temporally stable yield patterns associated with high EC_e and/or low P, are the reduction of N fertilizer in salt-affected zones and increase in P fertilizer once salinity issues are mitigated. Further studies are needed to test which precision management action will optimize net profitability in flood-irrigated rice systems in an environmentally sustainable manner.

Acknowledgments This research was supported by the Kearney Foundation of Soil Science; William G. and Kathleen Golden International Agriculture Fellowship; Henry A. Jastro Graduate Research Award; D. Marlin Brandon Rice Research Fellowship; and the Ben A. Madson Scholarship. Additionally, the research of J.M. Peña-Barragan was granted by the Fulbright-MEC postdoctoral program, financed by the Secretariat of State for Research of the Spanish Ministry for Science and Innovation. We thank the cooperating growers, George Tibbitts, Larry Maben and Charley Mathews for allowing us to conduct research on their farms. We are very grateful to the Agroecosystems Lab Manager, Cesar Abrenilla, as well as Kristen Kammeier, Denia Rodriguez Piza, Tim Doane, Ligia Azevedo, Bob Rousseau and numerous members of the Agroecosystems Lab at UC Davis for their assistance in the field and lab.

References

Bakhsh, A., Jaynes, D. B., Colvin, T. S., & Kanwar, R. S. (2000). Spatio-temporal analysis of yield variability for a corn-soybean field in Iowa. *Transactions of the ASAE, 43*(1), 31–38.

Basso, B., Bertocco, M., Sartori, L., & Martin, E. C. (2007). Analyzing the effects of climate variability on spatial pattern of yield in a maize–wheat–soybean rotation. *European Journal of Agronomy, 26*(2), 82–91.

Bivand, R., Altman, M., Anselin, L., Assunção, R., Berke, O., Bernat, A., et al. (2010). *Spdep: spatial dependence: weighting schemes, statisitics and models*. R package version 0.5-21. http://CRAN.R-project.org/package=spdep. Accessed 31 Aug 2010.

Brye, K. R. (2006). Soil biochemical properties as affected by land leveling in a clayey aquert. *Soil Science Society of America Journal, 70*(4), 1129–1139.

Burt, R. (2004). *Soil survey laboratory methods manual. SSIR No. 42, Version 4.0. NRCS-USDA*. Washington, DC: U.S. Government Printing Office.

Casanova, D., Goudriaan, J., Bouma, J., & Epema, G. F. (1999). Yield gap analysis in relation to soil properties in direct-seeded flooded rice. *Geoderma, 91*(3–4), 191–216.

Cassman, K. G. (1999). Ecological intensification of cereal production systems: Yield potential, soil quality, and precision agriculture. *Proceedings of the National Academy of Sciences, USA, 96*(11), 5952–5959.

Clesceri, L. S., Greenberg, A. E., & Eaton, A. D. (Eds.). (1998). *Standard methods for the examination of water and wastewater, flow injection analysis for orthophosphate (method 4500-P G)* (20th ed., pp. 4-149–4-150). Washington, DC: American Public Health Association.

De Datta, S. K., & Mikkelson, D. S. (1985). Potassium nutrition of rice. In R. D. Munson (Ed.), *Potassium in Agriculture* (pp. 665–669). Madison, WI: ASA, CSSA, and SSSA.

Delmotte, S., Tittonell, P., Mouret, J. C., Hammond, R., & Lopez-Ridaura, S. (2011). On farm assessment of rice yield variability and productivity gaps between organic and conventional cropping systems under mediterranean climate. *European Journal of Agronomy, 35*(4), 223–236.

Dimitriadou, E., Hornik, K., Leisch, F., Meyer, D., & Weingessel, A. (2010). *e1071: Misc functions of the department of statistics (e1071), TU Wien*. R package version 1.5-24. http://CRAN.R-project.org/package=e1071. Accessed 15 Feb 2012.

Doane, T. A., & Horwath, W. R. (2003). Spectrophotometric determination of nitrate with a single reagent. *Analytical Letters, 36*(12), 2713–2722.

Dobermann, A. (1994). Factors causing field variation of direct-seeded flooded rice. *Geoderma, 62*(1–3), 125–150.

Eck, H. V. (1987). Characteristics of exposed subsoil—at exposure and 23 years later. *Agronomy Journal, 79*(6), 1067–1073.

Flowers, T. J., & Yeo, A. R. (1981). Variability in the resistance of sodium chloride within rice (*Oryza sativa* L.) varieties. *New Phytologist, 88*(2), 863–1373.

Forster, J. C. (1995). Soil nitrogen. In K. Alef & P. Nannipieri (Eds.), *Methods in applied soil microbiology and biochemistry* (pp. 79–87). New York: Academic Press.

Guastaferro, F., Castrignanó, A., De Benedetto, D., Sollitto, D., Troccoli, A., & Cafarelli, B. (2010). A comparison of different algorithms for the delineation of management zones. *Precision Agriculture, 11*(6), 600–620.

Harris, D., Horwath, W. R., & van Kessel, C. (2001). Acid fumigation of soils to remove carbonates prior to total organic carbon or CARBON-13 isotopic analysis. *Soil Science Society of America Journal, 65*(6), 1853–1856.

Hofer, S. (2003). *Determination of ammonia (salicylate) in 2 M KCl soil extracts by flow injection analysis. QuikChem method 12-107-06-2-A*. Loveland: Lachat Instruments.

Khatun, S., & Flowers, T. J. (1995). Effects of salinity on seed set in rice. *Plant, Cell and Environment, 18*(1), 61–67.

Knepel, K. (2003). *Determination of nitrate in 2 M KCl soil extracts by flow injection analysis. QuikChem method 12-107-04-1-B*. Loveland: Lachat Instruments.

Lark, R. M., & Stafford, J. V. (1997). Classification as a first step in the interpretation of temporal and spatial variation of crop yield. *Annals of Applied Biology, 130*(1), 111–121.

Linquist, B., & Ruark, M. (2011). Re-evaluating diagnostic phosphorus tests for rice systems based on soil phosphorus fractions and field level budgets. *Agronomy Journal, 103*(2), 501–508.

Lutts, S., Kinet, J. M., & Bouharmont, J. (1995). Changes in plant response to NaCl during development of rice (*Oryza sativa* L.) varieties differing in salinity resistance. *Journal of Experimental Botany, 46*(12), 1843–1852.

Maas, E. V. (1990). Crop salt tolerance. In K. K. Tanji (Ed.), *Agricultural salinity assessment and management manual* (pp. 262–304). New York: American Society of Civil Engineers (ASCE) Manuals & Reports on Engineering Practices No. 71.

Maas, E. V., & Grattan, S. R. (1999). Crop yields as affected by salinity. In R. W. Skaggs & J. van Schilfgaarde (Eds.), *Agricultural drainage. Agronomy Monograph No. 38* (pp. 55–108). Madison, WI: ASA and SSSA.

Maas, E. V., & Hoffman, G. J. (1977). Crop salt tolerance—current assessment. *Journal of Irrigation and Drainage Engineering, American Society of Civil Engineers, 103*(2), 115–134.

Miranda, K. M., Espey, M. G., & Wink, D. A. (2001). A rapid, simple spectrophotometric method for simultaneous detection of nitrate and nitrite. *Nitric Oxide, 5*(1), 62–71.

Mzuku, M., Khosla, R., Reich, R., Inman, D., Smith, F., & MacDonald, L. (2005). Spatial variability of measured soil properties across site-specific management zones. *Soil Science Society of America Journal, 69*(5), 1572–1579.

Olsen, S. R., & Sommers, L. E. (1982). Phosphorus. In A. L. Page, R. H. Miller, & D. R. Keeney (Eds.), *Methods of soil analysis, Part 2: Chemical and microbiological properties. Agronomy Mongraph No. 9* (2nd ed., pp. 403–430). Madison, WI: ASA and SSSA.

Perez-Quezada, J. F., Pettygrove, G. S., & Plant, R. E. (2003). Spatial-temporal analysis of yield and the influence of soil factors in two four-crop-rotation fields in the Sacramento Valley, California. *Agronomy Journal, 95*(3), 676–687.

Raney, F. C., Hagan, R. M., & Finfrock, D. C. (1957). Water temperature in irrigation. *California Agriculture, 11*(4), 19–20.

Rao, P. S., Mishra, B., Gupta, S. R., & Rathore, A. (2008). Reproductive stage tolerance to salinity and alkalinity stresses in rice genotypes. *Plant Breeding, 127*(3), 256–261.

Maclean, J. L., Dawe, D. C., Hardy, B., & Hettel, G. P. (Eds.). (2002). *Rice almanac* (3rd ed). Wallingford: CABI Publishing and Los Baños.

Roel, A., Mutters, R. G., Eckert, J. W., & Plant, R. E. (2005). Effect of low water temperature on rice yield in California. *Agronomy Journal, 97*(3), 943–948.

Roel, A., & Plant, R. E. (2004a). Spatiotemporal analysis of rice yield variability in two California fields. *Agronomy Journal, 96*(1), 77–90.

Roel, A., & Plant, R. E. (2004b). Factors underlying yield variability in two California rice fields. *Agronomy Journal, 96*(5), 1481–1494.

Scardaci, S. C., Shannon, M. C., Grattan, S. R., Eke, A. U., Roberts, S. R., Goldman-Smith, S., et al. (2002). Water management practices can affect salinity in rice fields. *California Agriculture, 56*(6), 184–188.

Shannon, M. C., Rhoades, J. D., Draper, J. H., Scardaci, S. C., & Spyres, M. D. (1998). Assessment of salt tolerance in rice cultivars in response to salinity problems in California. *Crop Science, 38*(2), 394–398.

Shimono, H. T., Hasegawa, T., Fujimura, S., & Iwama, K. (2004). Responses of leaf photosynthesis and plant water status in rice to low water temperature at different growth stages. *Field Crops Research, 89*(1), 71–83.

Shimono, H. T., Hasegawa, T., & Iwama, K. (2002). Responses of growth and grain yield in paddy rice to cool water at different growth stages. *Field Crops Research, 73*(2–3), 67–79.

Shimono, H., Okada, M., Kanda, E., & Arakawa, I. (2007). Low temperature-induced sterility in rice: Evidence for the effects of temperature before panicle initiation. *Field Crops Research, 101*(2), 221–231.

Therneau, T. M., & Atkinson, B. (2009). *R port by brian ripley. rpart: recursive partitioning*. R package version 3.1-45. http://CRAN.R-project.org/package=rpart. Accessed 15 Feb 2012.

Thomas, G. W. (1982). Exchangeable cations. In A. L. Page, R. H. Miller, & D. R. Keeney (Eds.), *Methods of soil analysis: Part 2. Chemical and microbiological properties. Agronomy monograph 9* (2nd ed., pp. 159–165). Madison, WI: ASA and SSSA.

U.S. Environmental Protection Agency Method 200.7. (2001). *Trace elements in water, solids, and biosolids by inductively coupled plasma-atomic emission spectrometry*. Washington, DC: U.S. EPA.

Verdouw, H., Van Echteld, C. J. A., & Dekkers, E. M. J. (1978). Ammonia determination based on indophenol formation with sodium salicylate. *Water Research, 12*(6), 399–402.

Waggoner, P. E., & Aylor, D. E. (2000). Epidemiology, a science of patterns. *Annual Review of Phytopathology, 38*(1), 71–94.

Walker, T. W., Kingery, W. L., Street, J., Cox, M. S., Oldham, J. L., Gerard, P. D., et al. (2003). Rice yield and soil chemical properties as affected by precision land-leveling in alluvial soils. *Agronomy Journal, 95*(6), 1483–1488.

Wehlan, B. M., & McBratney, A. B. (2000). The "null hypothesis" of precision agriculture management. *Precision Agriculture, 2*(3), 265–279.

Williams, J. F. (2010). *Rice nutrient management in California. Publ. 3516*. California: University of California, Agriculture and Natural Resources.

Yanai, J., Lee, C. K., Kaho, T., Iida, M., Matsui, T., Umeda, M., et al. (2001). Geostatistical analysis of soil chemical properties and rice yield in a paddy field and application to the analysis of yield-determining factors. *Soil Science and Plant Nutrition, 47*(2), 291–301.